

Title	Transport, atom blockade, and output coupling in a Tonks-Girardeau gas
Authors	Rutherford, L.;Goold, John;Busch, Thomas;McCann, J. F.
Publication date	2011
Original Citation	Rutherford, L., Goold, J., Busch, T. and McCann, J. F. (2011) 'Transport, atom blockade, and output coupling in a Tonks-Girardeau gas', Physical Review A, 83(5), 055601 (4pp). doi: 10.1103/PhysRevA.83.055601
Type of publication	Article (peer-reviewed)
Link to publisher's version	https://journals.aps.org/pr/abstract/10.1103/PhysRevA.83.055601 - 10.1103/PhysRevA.83.055601
Rights	© 2011, American Physical Society
Download date	2023-09-30 20:10:06
Item downloaded from	https://hdl.handle.net/10468/4511



UCC

University College Cork, Ireland
 Coláiste na hOllscoile Corcaigh

Transport, atom blockade, and output coupling in a Tonks-Girardeau gas

L. Rutherford,¹ J. Goold,^{2,3} Th. Busch,³ and J. F. McCann¹

¹*Centre for Theoretical Atomic, Molecular and Optical Physics, Queen's University Belfast, Belfast BT7 1NN, United Kingdom*

²*Clarendon Laboratory, University of Oxford, Oxford, United Kingdom*

³*Physics Department, University College Cork, Cork, Ireland*

(Received 23 November 2010; revised manuscript received 11 February 2011; published 31 May 2011)

Recent experiments have demonstrated how quantum-mechanical impurities can be created within strongly correlated quantum gases and used to probe the coherence properties of these systems [S. Palzer, C. Zipkes, C. Sias, and M. Köhl, *Phys. Rev. Lett.* **103**, 150601 (2009)]. Here we present a phenomenological model to simulate such an output coupler for a Tonks-Girardeau gas that shows qualitative agreement with the experimental results for atom transport and output coupling. Our model allows us to explore nonequilibrium transport phenomena in ultracold quantum gases and leads us to predict a regime of atom blockade, where the impurity component becomes localized in the parent cloud despite the presence of gravity. We show that this provides a stable mixed-species quantum gas in the strongly correlated limit.

DOI: 10.1103/PhysRevA.83.055601

PACS number(s): 03.75.Hh, 67.10.Jn, 05.60.Gg

Ultracold gases provide an extremely versatile resource of quantum matter. The possibility of applying external electromagnetic potentials means that one can create macroscopic harmonic traps and microscopic periodic structures that are sensitive to the quantum states of the atomic species [1]. One recent breakthrough has been the realization that quasi-one-dimensional quantum degenerate gases can be created by using strong transverse trapping potentials [2]. Such settings allow the radial (transverse) degrees of freedom to be frozen out and in addition to tune the effective one-dimensional interaction strength [3]. The resulting quantum many-body system of interacting bosons can be described by the Lieb-Liniger model, which possesses exact solutions [4]. In the limit of strong repulsive interactions these can be simplified due to the existence of a mapping theorem to an equivalent gas of noninteracting fermions [5]. This so-called Tonks-Girardeau (TG) limit was recently experimentally reached independently in two separate laboratories [6,7] and the initial experiments were followed by several spectacular experimental studies. These included the exploration of the relationship between integrability and thermalization [8] and also the creation and detection of metastable excited states [9].

Very recently Palzer *et al.* [10] demonstrated an output coupler for an optically trapped quantum gas in the TG regime. An array of one-dimensional clouds was created in a two-dimensional optical lattice and then probed using a radio-frequency pulse to locally populate an untrapped hyperfine level. The transport properties of this untrapped “impurity” as it fell under gravity, passing through the parent cloud, were subsequently observed. This experiment constitutes a genuine open quantum system and also one of the first experiments that explores the important topic of quantum transport in a clean ultracold environment (see also [11]). Here we propose a theoretical framework that can describe the effects experimentally observed and predict the existence of a regime of atom blockade, in which the interaction between two components is strong enough to trap and localize the impurity state. This phenomenon of self-trapping of neutral impurity atoms in quantum degenerate gases has received a significant amount of theoretical attention in recent times

[12–14] and our description paves the way for an immediate experimental realization of the effect in this one-dimensional configuration. Moreover, our work complements and extends recent theoretical interest in the area of general impurity embedding in the Tonks-Girardeau regime [15–17].

A low-density gas of N identical bosons trapped in a quasi-one-dimensional waveguide can be described by the Hamiltonian

$$\mathcal{H} = \sum_{i=1}^N \left[\frac{-\hbar^2}{2m} \frac{\partial^2}{\partial z_i^2} + V(z_i) \right] + \kappa \sum_{i < j} \delta(|z_i - z_j|), \quad (1)$$

where m is the mass of the particles, z the axial coordinate, and $V(z_i) = \frac{1}{2}m\omega_{\parallel}^2 z_i^2$ is the axial trapping potential, with ω_{\parallel} the corresponding axial angular frequency and a_{\parallel} is the corresponding trap length. The strength of the atom-atom contact interactions is given by κ , the one-dimensional coupling constant, which can be derived by a renormalization procedure from the three-dimensional scattering process as $\kappa = \frac{4\hbar^2 a_{3D}}{ma_{\perp}} (a_{\perp} - Ca_{3D})^{-1}$ [3]. Here $a_{\perp} = \sqrt{\hbar/m\omega_{\perp}}$ is the radial trap width and ω_{\perp} the radial trapping frequency. The standard s -wave scattering length is denoted by a_{3D} and $C \approx 1.4603$. For the ^{87}Rb isotope we have $a_{3D} \approx 5.3 \times 10^{-9}$ m for both hyperfine states used in [10], and $m \approx 1.44 \times 10^{-25}$ kg. For finite κ the Hamiltonian describes an inhomogeneous Lieb-Liniger gas and we characterize the strongly interacting regime by demanding that the contact interaction dominates the kinetic energy $\kappa \gg \hbar^2 n_{1D}/m$, where n_{1D} is the mean linear density of the atoms. In this limit the many-body problem admits a unique and particularly elegant solution, as it allows one to replace the contact interaction in Eq. (1) with the nodal boundary condition $\Psi_B(z_1, z_2, \dots, z_N, t) = 0$ if $|z_i - z_j| = 0$, for $i \neq j$ and $1 \leq i \leq j \leq N$. Such a constraint can be enforced *a priori* by Slater determinant factorization, $\Psi_F(z_1, z_2, \dots, z_N, t) = \frac{1}{\sqrt{N!}} \det_{(n,j)=(0,1)}^{(N-1,N)} \psi_n(z_j, t)$, where the ψ_n are the single-particle eigenstates of the *noninteracting* system. We have adopted the convention of labeling the first N single-particle eigenfunctions with the index $n = 0, 1, 2, \dots, N-1$. This, however, leads to a fermionic rather than bosonic exchange symmetry, which is corrected by

proper symmetrization, $A = \prod_{1 \leq i < j \leq N} \text{sgn}(z_i - z_j)$ to give $\Psi_B = A \Psi_F$ [5]. From this exact solution, the time-dependent single-particle density is given by [18,20]

$$\begin{aligned} \rho(z, t) &= N \int_{-\infty}^{+\infty} |\Psi_B(z, z_2, \dots, z_N; t)|^2 dz_2 \dots dz_N \\ &= \sum_{n=0}^{N-1} |\psi_n(z, t)|^2. \end{aligned} \quad (2)$$

In the experiment by Palzer *et al.* [10] an array of one-dimensional clouds was created with the axis vertically aligned. A localized excitation of a small section (near the center) of the cloud to an untrapped hyperfine state was introduced. While these untrapped atoms fall under gravity, they remain strongly confined in the transverse direction created by the optical fields. The dynamics of the system can therefore be split into the description of its two components: a trapped background gas of initially N_b atoms, and an impurity wave packet of N_i atoms, with atom densities $\rho_b(z, t)$ and $\rho_i(z, t)$, respectively.

Girardeau originally used his famous mapping theorem to find the unique solution to the single component many-body problem. The solution of the full time-dependent two-component many-body problem is challenging and only a small number of exact solutions exist for time-independent mixtures [19]. Here we suggest that a two-component system with transport can be treated using a phenomenological approach based on the time evolution of nonlinearly coupled single particle states. The density distributions are then built from these states by assuming single component Tonks-Girardeau gases for both the impurity and parent components [see Eq. (2)].

At time $t = 0$, all atoms in the system are assumed to be in the trapped TG gas state, the density of which can be calculated without approximation using Eq. (2). We then simulate the experiment through the application of a short, broadband pulse, $f(z, t)$, with a Gaussian spatial intensity of FWHM $\sigma = 2.3 \mu\text{m}$, for a duration of $t_{\text{pulse}} = 200 \mu\text{s}$. The intensity of this pulse, γ , is chosen such that the population transfer corresponds to the experimental situation in which, on average, three atoms were coupled out [10]. The integrated densities (norms) of the two components vary in time and according to a set of coupled nonlinear Schrödinger equations of the form

$$\begin{aligned} i\hbar \frac{\partial \psi_n}{\partial t} &= \left[-\frac{\hbar^2}{2m} \frac{\partial^2}{\partial z^2} + \frac{1}{2} m \omega_{\parallel}^2 z^2 + \kappa \rho_i \right] \psi_n + \gamma f(z, t) \phi_n, \\ i\hbar \frac{\partial \phi_n}{\partial t} &= \left[-\frac{\hbar^2}{2m} \frac{\partial^2}{\partial z^2} + mgz + \kappa \rho_b \right] \phi_n + \gamma f(z, t) \psi_n. \end{aligned} \quad (3)$$

The densities of the impurity and background components are then built according to $\rho_b(z, t) = \sum_{n=0}^{N-1} |\psi_n(z, t)|^2$ and $\rho_i(z, t) = \sum_{n=0}^{N-1} |\phi_n(z, t)|^2$, respectively. Here g is the gravitational acceleration and we have assumed that the inter-component scattering is in mean-field regime. This can be justified by realizing that the impenetrability of the nonlike atoms in the Tonks limit is overcome by the gravitational pull on the impurity, which leads to an increase in the scattering parameter $k|a_{1D}|$, where k is the linear atomic momentum and a_{1D} is the atomic scattering length. In this regime the collisions

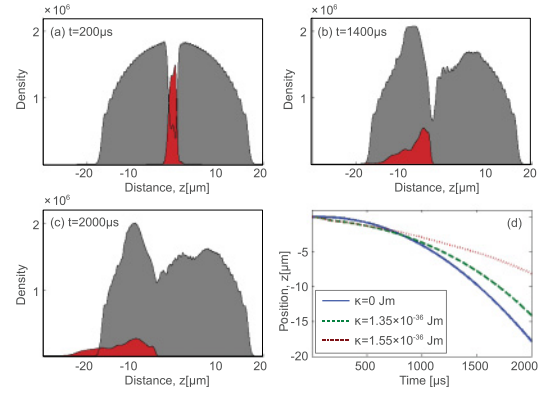


FIG. 1. (Color online) Density profiles of the two-component Tonks gas system for different times (a) $t = 200 \mu\text{s}$, (b) $t = 1400 \mu\text{s}$, and (c) $t = 2000 \mu\text{s}$ for $N_b = 50$ ^{87}Rb atoms and $\omega_{\parallel} = 2\pi \times 39 \text{ Hz}$. The gray (lighter) curves show the trapped component, while the red (darker) curves show the impurity wave packet. The width of the out-coupling pulse is $\sigma = 2.3 \mu\text{m}$ and the intercomponent interaction strength is $\kappa = 1.35 \times 10^{-36} \text{ Jm}$. (d) shows the center-of-mass trajectory of the impurity atoms for different interaction strengths κ .

between particles in different states can no longer be treated as collisions between impenetrable particles. The strength of this scattering, κ , is calculated from the data given in [10] to be $\kappa \sim 1.35 \times 10^{-36} \text{ Jm}$. In the following we will show results from simulating these coupled equations for a gas of initially $N_b = 50$ atoms, from which the out-coupling process transfers $N_i \approx 3$ into the impurity. All parameters are chosen such that a direct, qualitative comparison to the experiment is possible [10].

The densities of the components after the out-coupling process and during the subsequent dynamics are shown in Fig. 1. Initially, after the coupling pulse is switched off ($t = 200 \mu\text{s}$), the impurity component is localized at the origin ($z = 0 \mu\text{m}$) and subsequently disperses and displaces as it is dragged through the trapped component by gravity ($t = 1400 \mu\text{s}$ and $t = 2000 \mu\text{s}$). The response of the background cloud on these timescales is mainly determined by the interaction with the falling impurity and our results agree qualitatively well with the experimental findings of Palzer *et al.* [10]. This provides support for our specific phenomenological model, as other approaches, for example assuming coherence within the impurity, led to a dynamics that agreed very poorly.

The transport process was studied by analysis of the impurity's center-of-mass motion, which is shown in Fig. 1(d) for three different values of the interaction strength, κ . It can be seen that a finite interaction produces noticeable deviations from parabolic flight. Firstly, the center-of-mass is expelled downward, on a very short time scale. This can be understood by realizing that the resonance position for the coupling is moved toward negative z values for increasing magnitude of the nonlinear terms in Eq. (3) (see also discussion below). After this the fall of the out-coupled atoms is slowed by the trapped cloud as compared to the free-fall case. We find that for $\kappa = 1.35 \times 10^{-36} \text{ Jm}$ eventually all atoms exit the overlap region with the trapped component, however the

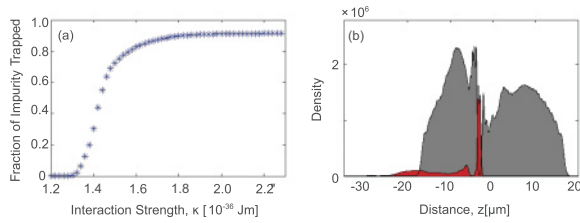


FIG. 2. (Color online) (a) Atom blockade: shown is the fraction of out-coupled atoms remaining within the confines of the trapped gas after $t = 3000 \mu\text{s}$. (b) Density profile taken at $t = 2000 \mu\text{s}$ for a gas in the intermediate regime at $\kappa = 1.44 \times 10^{-36} \text{ Jm}$.

significant slowdown for $\kappa = 1.55 \times 10^{-36} \text{ Jm}$ points toward the interesting possibility of blockade within the gas.

Being able to trap the impurity and leave it embedded in the parent cloud is an exciting prospect for a novel mixed quantum gas. We therefore calculate the fraction of impurity atoms that might be retained within the confines of the trapped cloud ($[-20, 20] \mu\text{m}$) after $3000 \mu\text{s}$. In each case approximately three atoms are present in the impurity wave packet and Fig. 2(a) shows how the fraction remaining within the cloud region varies as a function of κ . Three regimes can be identified: (i) at interaction strengths below $\kappa \approx 1.35 \times 10^{-36} \text{ Jm}$ the entire impurity wave packet is able to pass through the trapped component and exit the cloud; (ii) in the region between $\kappa \approx 1.35 \times 10^{-36} \text{ Jm}$ and $\kappa \approx 1.5 \times 10^{-36} \text{ Jm}$ the impurity wave packet splits into two components of which one leaves the cloud and the other remains trapped in the center; and (iii) above $\kappa \approx 1.5 \times 10^{-36} \text{ Jm}$ maximum self-trapping is achieved, with $>90\%$ of the atomic density blockaded inside the trapped gas for long timescales. A typical density plot for an interaction strength in the intermediate regime ($\kappa = 1.44 \times 10^{-36} \text{ Jm}$) after $2000 \mu\text{s}$ is shown in Fig. 2(b). Approximately half of the out-coupled density is clearly visible to be localized in the center of the background gas, while the other half has been significantly accelerated by gravity. This part will continue to travel out of the cloud.

Let us in the following consider the effects due to the asymmetry induced by the gravitational potential. For this we look at the situation in which the center of the out-coupling pulse is located away from the origin of the harmonic potential. Figure 3(a) shows the results for the number of out-coupled atoms when the pulse is focused around $z_0 = \pm 6 \mu\text{m}$. One immediately notes that the out-coupling yield at both positions is dramatically reduced in comparison with coupling from the center. While this can be partly explained by the lower density of the TG gas at $z = \pm 6 \mu\text{m}$, it alone is not sufficient for the dramatic reduction. In fact, the low efficiency is due to the increasingly off-resonant nature of the out-coupling process for larger distances from the center, which stems from the presence of the strong gravitational potential in the out-coupled channel. This is also consistent with the increased value of the Rabi frequency as can be seen from Fig. 3(a) for $z_0 = 6 \mu\text{m}$. In fact, carrying out simulations for a system in which the strength of gravity can be decreased (corresponding to the optical lattice being rotated from vertical to horizontal), shows in increase in Rabi frequencies with decreasing detuning between the channels [see Fig. 3(b)]. Note that while during the time of

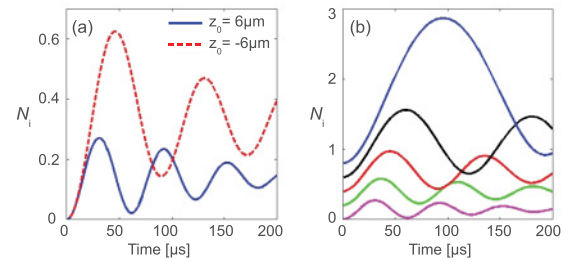


FIG. 3. (Color online) Output yield for a pulse of duration $t_{\text{pulse}} = 200 \mu\text{s}$. (a) shows the asymmetry present when the focus of the pulse is offset by a distance $z_0 = \pm 6 \mu\text{m}$ from the center of the cloud. (b) shows how the frequency of the Rabi oscillations (at $z_0 = 6 \mu\text{m}$) are affected for different strength of gravity, $g_{\text{eff}}/g = 0.2, 0.4, 0.6, 0.8, 1$ corresponding to the curves from top to bottom. The curves are vertically offset for clarity by $\Delta N = 0.2$. Note that the justification for the nonlinear term in Eq. (3) requires a finite gravitational strength.

the out-coupling process the gravitational pull has only a small effect on the position of the out-coupled atoms, the dephasing of the output can already be seen in the damping of the Rabi oscillations.

To understand the yield variations observed in Fig. 3(a) let us, in the following, investigate the reaction of the system to a change in the width, σ , of the out-coupling pulse. In the middle panel of Fig. 4 we show the output yield at the end of the coupling pulse ($t = 200 \mu\text{s}$) as a function of the position of the focal point for a pulse of the experimental FWHM of $\sigma = 2.3 \mu\text{m}$. Focusing on or close to the center of the trap ensures the expected large efficiencies, and the strong asymmetry observed in Fig. 3(a) becomes visible for increasing values of $|z_0|$. The visible fine structure is due to the existence of Rabi oscillations. The strong fall-off away from the trap centre shows that the effect of gravitational detuning is important over the scale of a few microns and therefore can be important over the spatial profile of the out-coupling pulse. It will, in particular, influence the coherence of the coupling process and we show in the left and right panels of Fig. 4 that an increase of the pulse width, σ , leads to a decay of the coherent, high-contrast Rabi oscillations. The fact that for out-coupling pulses of the same duration the number of oscillations visible for small values of σ is different for coupling above and below the cloud centre can be understood by remembering that the resonance point is below the the trap center. Therefore the

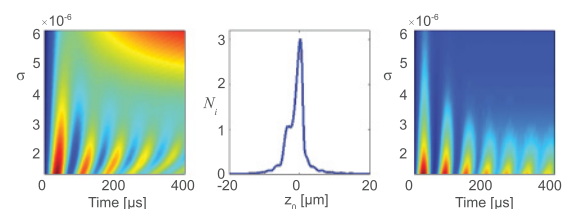


FIG. 4. (Color online) The effect of pulse width σ on the atom output yield from a TG gas below and above the center of the trap. Left: Atom yield for a pulse focused at $z_0 = -6 \mu\text{m}$. Center: Output yield (at the end of the pulse) as a function of focal point for $\sigma = 2.3 \mu\text{m}$. Right: Yield for focus at $z_0 = 6 \mu\text{m}$. Well-defined Rabi oscillations are clearly visible for small σ for for both situations, above (right) and below (left) the trap center.

detuning at positive z_0 is larger than at negative z_0 , leading to higher frequency oscillations.

As the spot size increases the detuning gradient gives rise to different phase components in the out-coupled pulse, which leads to the vanishing of the Rabi oscillations. This is also the reason for the displacement of the oscillations with increasing spot size, as broader spots are able to sample areas closer to the resonance (which for our parameters lies at $z_R = -1.9 \mu\text{m}$) with lower Rabi frequency. As the spot size increases further a pulse at $z_0 = -6 \mu\text{m}$ significantly overlaps with the resonance point and its output becomes dominated by a single (coherent) component from the high-density central region of the trap. This leads to the increase observed in the upper right hand side corner of the left panel of Fig. 4. While the spot size for the out-coupling pulse cannot be made arbitrarily small, these effects could be experimentally observed by weakening the longitudinal trapping, for example.

In conclusion, we have presented a model for transport in strongly correlated quantum gases that is able to reproduce key features of recent experiments. Furthermore, our model predicts several features which could be explored further

experimentally. We have brought strong evidences that even in the presence of gravity a strong interaction between an out-coupled and a residing component in a Tonks gas can lead to a self-localization of the out-coupled component. Although atom blockade was not observed in the experiment of Palzer *et al.*, the regime could be reached by tuning a Feshbach resonance between the hyperfine states. In addition our work has shed light on interesting aspects of the out coupling process which are unique to the configuration under consideration. Using our model to investigate other condensed matter phenomena in these correlated systems, such as spin-charge separation and analogues of Cherenkov radiation, are subjects of ongoing research.

L.R. is grateful to the Department for Employment and Learning (Northern Ireland) for financial support. The work was supported by Science Foundation Ireland under project nos. 05/IN/I852 and 05/IN/I852 NS. J.G. would like to acknowledge funding from an IRCSET Marie Curie International Mobility grant. J.G. and T.B. would like to thank A. del Campo for interesting discussions.

-
- [1] I. Bloch, J. Dalibard, and W. Zwerger, *Rev. Mod. Phys.* **80**, 885 (2008).
- [2] H. Moritz, T. Stöferle, M. Köhl, and T. Esslinger, *Phys. Rev. Lett.* **91**, 250402 (2003).
- [3] M. Olshani, *Phys. Rev. Lett.* **81**, 938 (1998).
- [4] E. Lieb and W. Liniger, *Phys. Rev.* **130**, 1605 (1963).
- [5] M. Girardeau, *J. Math. Phys.* **1**, 516 (1960).
- [6] B. Paredes, A. Widera, V. Murg, O. Mandel, S. Fölling, I. Cirac, G. V. Shlyapnikov, T. W. Hänsch, and I. Bloch, *Nature (London)* **429**, 277 (2004).
- [7] T. Kinoshita, T. Wenger, and D. S. Weiss, *Science* **305**, 1125 (2004).
- [8] T. Kinoshita, T. Wenger, and D. S. Weiss, *Nature (London)* **440**, 900 (2006).
- [9] E. Haller, M. Gustavsson, M. J. Mark, J. G. Danzl, R. Hart, G. Pupillo, and H. C. Nägerl, *Science* **325**, 1224 (2009).
- [10] S. Palzer, C. Zipkes, C. Sias, and M. Köhl, *Phys. Rev. Lett.* **103**, 150601 (2009).
- [11] C. D. Fertig, K. M. O'Hara, J. H. Huckans, S. L. Rolston, W. D. Phillips, and J. V. Porto, *Phys. Rev. Lett.* **94**, 120403 (2005).
- [12] F. M. Cucchietti and E. Timmermans, *Phys. Rev. Lett.* **96**, 210401 (2006).
- [13] Ryan M. Kalas and D. Blume, *Phys. Rev. A* **73**, 043608 (2006).
- [14] M. Bruderer, W. Bao, and D. Jaksch, *Europhys. Lett.* **82**, 30004 (2008).
- [15] J. Goold and Th. Busch, *Phys. Rev. A* **77**, 063601 (2008).
- [16] M. D. Girardeau and A. Minguzzi, *Phys. Rev. A* **79**, 033610 (2009).
- [17] J. Goold, H. Doerk, Z. Idziaszek, T. Calarco, and Th. Busch, *Phys. Rev. A* **81**, 041601 (2010).
- [18] V. I. Yukalov and M. D. Girardeau, *Laser Phys. Lett.* **2**, 375 (2005).
- [19] M. D. Girardeau and A. Minguzzi, *Phys. Rev. Lett.* **99**, 230402 (2007).
- [20] M. D. Girardeau and E. M. Wright, *Phys. Rev. Lett.* **84**, 5239 (2000).
- [21] M. Feit, J. A. Fleck Jr., and A. Steiger, *J. Comput. Phys.* **47**, 412 (1982).
- [22] M. D. Girardeau and A. Minguzzi, *Phys. Rev. A* **79**, 033610 (2009).